Environmental Science
Water Research & Technology

ROYAL SOCIETY OF CHEMISTRY

PAPER

View Article Online
View Journal | View Issue

Cite this: *Environ. Sci.: Water Res. Technol.*, 2023, **9**, 2942

Influence of colloidal iron oxide and natural organic matter fouling on nanofiltration membrane performance: role of feed composition and membrane properties†

Desislava Filipova Davidkova,[a] Margaret Graham,[b] Santiago Romero-Vargas Castrillón *[ac] and Andrea Joana Correia Semião*[a]

Membrane fouling is an inherent technical challenge in nanofiltration (NF) processes for drinking water production. The effect of various organic and inorganic foulants on membrane performance has been studied extensively, but mechanistic understanding of combined organic–inorganic fouling, notably of iron oxide and natural organic matter (NOM), is lacking. This study investigates iron (Fe) oxide colloidal fouling in the presence of NOM and compares its effect on the water and solute transport properties of two commercial NF membranes (polypiperazine amide NF270 *versus* cellulose acetate SBNF). Fe oxide alone caused no significant change (<5%) in permeate flux and ion rejection due to the high electrostatic double-layer repulsion force (F_{EDL}) between an initially deposited discontinuous foulant layer and colloids in the bulk feed solution. The presence of NOM caused surface charge reversal (from positive to negative) of the iron oxide colloids, leading to severe flux decline (30%) and salt rejection increase for the cellulose acetate membranes. A similar flux decline (30%) was observed in fouling experiments with NOM, suggesting that NOM is the determining factor in NOM–inorganic fouling. The polypiperazine amide membrane was less prone to fouling due to its higher hydrophilicity compared to cellulose acetate. However, reduced electrostatic double-layer repulsion force during combined fouling in the presence of Ca^{2+} led to significant flux loss (30%). This paper highlights the synergy between membrane surface properties and foulant chemistry in explaining NF fouling mechanisms.

Received 6th July 2023,
Accepted 9th September 2023

DOI: 10.1039/d3ew00495c

rsc.li/es-water

Water impact

Understanding the individual and combined effects of naturally-occurring foulants is imperative for improving nanofiltration (NF)-based drinking water treatment. We systematically investigate the fouling potential of stable iron oxide colloidal dispersions supplemented with natural organic matter (NOM). Charge reversal of the NOM-coated colloids and specific interactions with divalent ions, ubiquitous in feed surface waters, lead to irreversible flux loss regardless of NF membrane material type.

1. Introduction

Nanofiltration (NF) is a widely used membrane-based process for drinking water production due to its improved permeate water quality compared to ultrafiltration (UF), and lower energy consumption than reverse osmosis (RO).[1] Despite advances in membrane science, fouling remains a major technical obstacle in NF-based water treatment. Accumulation of organic, inorganic and biological substances on the membrane surface and inside the pores reduces the permeate flux, affects water quality and increases plant operating costs.[2]

Inorganic silica-, iron-, manganese- and aluminium-bearing deposits, which naturally occur in surface waters, have previously been detected on decommissioned membranes from drinking water treatment plants (DWTP).[3–5] This has motivated several studies to investigate the mechanisms behind NF membrane colloidal fouling through systematic laboratory tests with negatively-charged silica as

[a] *Institute for Infrastructure and Environment, School of Engineering, The University of Edinburgh, William Rankine Building, Thomas Bayes Road, Edinburgh EH9 3FG, UK. E-mail: Santiago@ed.ac.uk, Andrea.Semiao@ed.ac.uk*
[b] *School of Geosciences, The University of Edinburgh, Crew Building, Alexander Crum Brown Road, Edinburgh EH9 3FF, UK*
[c] *Institute for Materials and Processes, School of Engineering, The University of Edinburgh, Sanderson Building, Robert Stevenson Road, Edinburgh EH9 3FB, UK*
† Electronic supplementary information (ESI) available. See DOI: https://doi.org/10.1039/d3ew00495c

model inorganic foulant.[6–9] However, iron (Fe) and aluminium[10] (Al) colloids, which acquire a net positive surface charge at slightly acidic and near-neutral pH, have been overlooked. Despite the typically low Fe concentration in surface feed waters (0.25–3.5 mg L^{-1}),[11–13] its environmental cycling[14] ensures the continuous exposure of the membrane to colloidal Fe. In well-oxygenated surface waters, ferrous iron – Fe(II) – is converted to ferric, Fe(III), and can form insoluble colloidal (oxy)(hydro)oxide species.[14] As some membrane plants treating surface water in northern latitudes[12,15–17] do not use any form of pre-treatment (*e.g.*, flocculation and sedimentation), apart from coarse screening of the feed water (50–2000 μm), iron colloidal particles (<0.45 μm) are not removed and can hence build up on the membrane over time and decrease its useful life.[18] Two previous studies investigating iron colloidal fouling in RO membranes, have directly added soluble $FeCl_3$ or $Fe(OH)_3$ to the feed at the fouling onset, and assumed iron oxide particle formation at near-neutral pH.[19,20] The observed flux loss was between 7%[20] and 14%[19] after 7 hours of fouling depending on the operating conditions. However, those studies have pointed out that the colloidal iron system formed by the direct addition of iron salt to the feed is unstable,[19] which can lead to agglomeration and settling in the feed tank. Therefore, an improved protocol is needed to study the effect of *stable* iron oxide colloids and their properties (*e.g.*, size and zeta potential) on NF membrane performance.

In addition to inorganic colloidal foulants, natural organic matter (NOM) presents a major challenge for membrane processes in temperate regions such as North America and Northern Europe, where organic-rich soils result in moderate surface water total organic carbon (TOC) concentrations (2.2–14.6 mg C/L).[11,12,21–24] NOM molecules (primarily composed of fulvic acids, humic acids and some polysaccharides) have an overall negative surface charge at neutral pH due to carboxylic and phenolic functional groups.[25] Consequently, NOM fouling of NF membranes is strongly dependent on the pH, type and concentration of ions in solution, owing to electrostatic double-layer interactions and specific divalent complexation.[26] For instance, addition of Ca^{2+} worsens fouling by bridging carboxylic groups in adjacent organic molecules, which leads to a more compact foulant layer and up to five times more severe flux loss compared to organic fouling in the presence of Na^{+}.[27]

Since positively-charged inorganic colloids (such as aluminium and iron oxides) and NOM co-exist in natural surface waters, their interactions and combined fouling effect on NF membrane performance warrants systematic investigation. In the presence of NOM, adsorption of negatively-charged organics onto the positively-charged colloidal surface can cause charge neutralisation or reversal,[25,28] which affects membrane-foulant interactions. A study with oppositely-charged colloidal and organic foulants has been conducted by Mahlangu *et al.*[10] using aluminium oxides and sodium alginate (SA) (20 mg L^{-1}), a model organic foulant for biofilms, in polypiperazine amide NF270 membrane filtration experiments. The flux loss observed after 72 hours with mixed inorganic–organic foulants, was comparable to that observed with aluminium oxide alone: 17% and 15%, respectively.[10] However, the combined fouling in the presence of Ca^{2+}, led to the most severe flux loss (55%), due to Ca-bridging characteristic of organic-dominated fouling.[10] This suggests that in the presence of organics, the surface properties of the inorganic colloidal foulant are completely masked by the adsorbed SA, and the flux decline is determined by the organic foulant interactions.

Notwithstanding the existing research effort, there are no studies reporting the fouling behaviour of well-characterised (in terms of size and electrokinetic properties) stable iron oxide colloidal dispersions, and their interactions with NOM. In this paper we systematically investigate the fouling behaviour of the Fe oxide-NOM system; we explore the effects of divalent and monovalent cations on fouling severity to gain an improved understanding of the underlying fouling mechanisms, foulant-membrane and foulant-foulant interactions by testing two commercial polymeric NF membranes with different physico-chemical properties.

2. Materials and methods

2.1. NF membranes

Two commercial NF membranes were used: the cellulose acetate SBNF membrane (Trisep, USA), which is currently used in Scottish DWTPs[29] and the polypiperazine amide thin-film composite NF270 membrane (Dow, USA), which is commonly used in the literature.[9,30,31] These membranes were chosen to capture the fouling propensity of two NF membranes with distinct interfacial and transport properties. The NF270 membrane was supplied as a spiral-wound element, from which coupons were cut out. The SBNF membrane was supplied as a wet flatsheet. Both membranes were stored in ultrapure (UP) water at 5 °C in opaque Nalgene bottles prior to use, with weekly water change to avoid microbial growth and contamination. Membrane UP water (18.2 MΩ cm) permeance and conductivity rejection were measured for each coupon to ensure that intrinsic membrane properties did not differ by more than 15% between experiments. The permeance (A_0) was calculated from $A_0 = \frac{J_w}{TMP}$, where J_w is the UP water flux and TMP is transmembrane pressure difference. The conductivity rejection (R) was calculated from $= \left(1 - \frac{\sigma_p}{\sigma_f}\right) \times 100$, where σ_p and σ_f are the permeate and feed conductivities, respectively.

2.2. Foulants preparation and characterisation

Suwannee River natural organic matter (RO-concentrated) (SRNOM) (International Humic Substances Society) was used as model organic foulant. A stock solution (2 g L^{-1}) was prepared by dissolving the powdered SRNOM in ultrapure

water and stirring for 24 hours at room temperature.[26,32–35] The solution pH was adjusted to pH 5.5 using 1 M NaOH, and filtered through a 0.45 μm PVDF syringe filter (Kinesis, USA). The SRNOM stock solution was stored in a closed glass container at 4 °C in the dark and used within two months (Table S1†). The stock total organic carbon (TOC) concentration was redetermined before each fouling experiment using a TOC analyser (Shimadzu, Japan) and was found to not have changed within this time.

The inorganic iron oxide colloidal particles were prepared adapting the method by Burleson and Penn,[36] without microwave annealing. In brief, 40 mL of 0.48 M $NaHCO_3$ (Acros Organics) were added dropwise to 40 mL of 0.4 M $Fe(NO_3)_3$ (Acros Organics) over 50 minutes. The resulting solution was dialysed (Spectra/Por® MWCO 100–500 Da) at 4 °C against ultrapure water for 5 days, with the dialysis water changed 3 times a day. The product solution was stored in Falcon© tubes at room temperature and used within two months of preparation. A sample of the stock solution was used for determining the solid iron oxide concentration by centrifugation, freeze-drying and weighing. Separate stability experiments were undertaken to determine the pH and ionic strength yielding stable colloidal dispersions; these are presented in section S1 of the ESI.† Under the conditions chosen for this study (pH 5.5, I = 1 mM), negligible changes in colloid size occurred up to 72 hours after synthesis (Fig. S1†). Particle size and zeta potential were measured using a Zetasizer Nano ZS (Malvern Instruments Ltd.) dynamic light scattering analyser. All solutions were prepared with ultrapure (UP) grade (18.2 MΩ cm resistivity) water (Alto™ I Ultrapure water system, Triple Red Ltd.). Prior to use, all glassware was acid-washed and rinsed with ultrapure water.

2.3. Membrane test set-up

Experiments were carried out using a custom-built stainless steel, plate-and-frame crossflow membrane system. The system was operated in closed-loop mode, recycling the permeate and concentrate streams to the feed. The system was fitted with three Nalgene feed tanks to store the background electrolyte solution, foulant solution, and UP water used as cleaning solution. The feed solution was delivered by a diaphragm pump (P200 Hydra-Cell, UK) and equally split between 2 membrane cells (MMS, Switzerland), with feed channel dimensions 1 mm (height), 25 mm (width) and 191 mm (length). The membrane area is 0.0046 m^2. The inlet crossflow and permeate flow rates were monitored continuously using an oval gear flow meter (Macnaught, UK) and a flow sensor (SLF3S-1300F, Sensirion), respectively. The setup was also fitted with a temperature sensor (Pt100 Condustrie-Met AG, Germany) monitoring the temperature in the cells, and two pressure transducers (S model, Swagelok, UK) at the feed and permeate side. The flow rates, temperature and pressures were recorded using a DAQ55 data logger (Omega, UK), connected to a computer running the DaqViewer data acquisition software. The pressure was adjusted using a backpressure regulator (KPB Series, Swagelok, UK).

2.4. Fouling protocol

The membranes were compacted at 19–20 bar using UP water for at least 12 hours, and the pristine membrane permeance (A_0) was determined at 10 bar. Next, the background electrolyte was dosed into the feed tank to achieve a desired concentration of either 1 mM NaCl (Acros Organics) or 0.3 mM $CaCl_2$ (Acros Organics), while keeping the total ionic strength (I) constant at 1 mM. The low ionic strength of the solution (*e.g.*, 1 mM NaCl solution has conductivity of ~120 μS cm^{-1}) is typical of Scottish surface waters (76.9–170.7 μS cm^{-1}),[11] and ensures the stability of the iron oxide colloidal dispersion (see section S1†). The pH was 5.5 throughout the experiment. This pH was also chosen to guarantee the stability of the Fe oxide colloidal dispersion and hence keep consistent feed conditions throughout the experimental programme. The pressure was readjusted to reach the initial steady-state flux J_0 = 100 LMH while recirculating the background electrolyte solution for at least 3 hours (u = 0.234 m s^{-1}, Re = 450). The values for the parameters J_0 and u were chosen to accelerate fouling in lab scale experiments, as done in previous studies.[31,37] Next, the initial membrane conductivity rejection was determined in triplicate by measuring the feed (σ_f) and permeate (σ_p) conductivities using a hand-held conductivity meter (Oakton, USA). The foulant solution was prepared separately at twice (40 mg C/L and 80 mg L^{-1} Fe oxide) the experimental concentration by diluting the foulant stock solution with background electrolyte solution (either 1 mM NaCl or 0.3 mM $CaCl_2$) and adjusting the pH to 5.5. The foulant was stirred for 3–4 hours and then added to a second feed tank. Fouling was initiated by opening the valve of the second feed tank, at which point feed solution was drawn from the two feed tanks and the retentate was recirculated and split equally between the two tanks. This was carried out to avoid the emptying of one tank and entrainment of air bubbles in the system. A separate mixing experiment was done to ensure that under the hydrodynamic conditions considered, the foulant concentrations in the two feed tanks equalise within 30 minutes of recirculation to the desired experimental concentration (*i.e.*, 20 mg C/L and 40 mg L^{-1} Fe oxide) (data not shown). The high foulant concentrations in the feed were chosen to accelerate the fouling in laboratory conditions. After foulant addition to the system, the flux was monitored continuously for 24 hours, while the conductivity and TOC were sampled 1 h, 20 h and 23.5 h after initiation of the fouling experiment. A 15-minute cleaning of the membrane with UP water was done at the same crossflow velocity as applied during fouling (u = 0.234 m s^{-1}, Re = 450), and in the absence of applied pressure.[38,39] This step was employed to remove loosely-bound foulant layers and quantify the hydraulically

reversible flux decline. The normalised UP water membrane permeance (A/A_0) was calculated by dividing the permeance after cleaning (A) by the pristine membrane permeance (A_0) and was used to compare the severity of each foulant type. The temperature was set to 20 ± 1 °C throughout the experiment using a chiller (Haake, Germany). All experiments were run in duplicate. Results from individual experiments at each fouling condition can be found in Fig. S2–S5 in the ESI.†

2.5. Membrane characterisation techniques

Since no previously published peer-reviewed data was available, the molecular weight cut-off (MWCO) of the pristine SBNF membrane was determined experimentally in the crossflow set-up by measuring the TOC rejection of polyethylene glycol (PEG) of different molecular weight (600–10 000 g mol^{-1}) at TMP = 4 bar, u = 1.33 m s^{-1} (Re = 2555), and T = 20 °C. The MWCO of the NF270 was obtained from the literature.[40,41]

The surface zeta potential (ζ) of the pristine membranes was measured using an electrokinetic analyser (SurPASSIII, Anton Paar, Austria) over the pH range 2.6–8. Membrane hydrophobicity was characterised in terms of the water contact angle *via* the sessile drop method using a temperature-controlled goniometer (DSA30, Kruss) at 20 °C. Surface images and root-mean-squared roughness (R_{RMS}) values of the pristine membranes were obtained using tapping mode atomic force microscopy (AFM) (JPK NanoWizard 4XP, Bruker). Surface and cross-section morphology, along with elemental composition of the pristine and fouled membranes, were studied using scanning electron microscopy (Crossbeam 550 FIB-SEM, Zeiss) and energy-dispersive X-ray spectroscopy (XMax^N 150 detector, Oxford Instruments) (SEM–EDX). Further details on the sample preparation and membrane characterisation protocols are provided in section S2 of the ESI.†

3. Results and discussion

3.1. NF membranes characterisation

Membrane interfacial properties such as roughness, hydrophobicity and surface charge affect fouling severity.[42–45] Here we investigate the (hitherto uncharacterised) cellulose acetate SBNF membrane and compare it with another commercial NF membrane (NF270) (Fig. 1 and Table 1). The measured contact angle with water (38 ± 6.1°), zeta potential (from 14 to −21 mV for pH 2.6–8) and R_{RMS} (4.37 ± 1.87 nm) of the NF270 membrane were consistent with values found in the literature[40,41,46–50] (Fig. 1).

The low R_{RMS} (1.66 ± 0.45 nm) and relatively more hydrophobic surface (59.2 ± 2.7°) of the SBNF compared to the NF270 membrane agreed with properties of other cellulose acetate membranes.[51–54] Both membranes had negative surface charge at pH 5.5, which was the pH used in the fouling experiments: $\zeta \approx -10$ mV for the SBNF and $\zeta \approx -15$ mV for the NF270 (Fig. 1C). The negative charge of the polypiperazine amide NF270 membrane is due to deprotonation of carboxylic acid groups,[30,49] while for the cellulose acetate SBNF membrane, the surface charge arises from hydroxide (OH^-) ions adsorbed onto hydrophobic surface sites.[55] The R_{RMS} of either membrane was not affected by the type of background electrolyte present in the AFM fluid cell ($p > 0.05$, Fig. 1B), and although there is a significant difference in the R_{RMS} between the two membranes, with the SBNF having lower surface roughness ($p < 0.05$), both membranes are relatively smooth ($R_{RMS} < 10$ nm) (Fig. S8†).

The UP water permeance and solute rejection of the membranes were also investigated (Table 1). For the NF270 membrane these were comparable to previous studies.[40,46,56–58] The lower salt and TOC rejection of the SBNF membrane can be linked to its relatively high MWCO compared to that of the NF270 (Table 1).

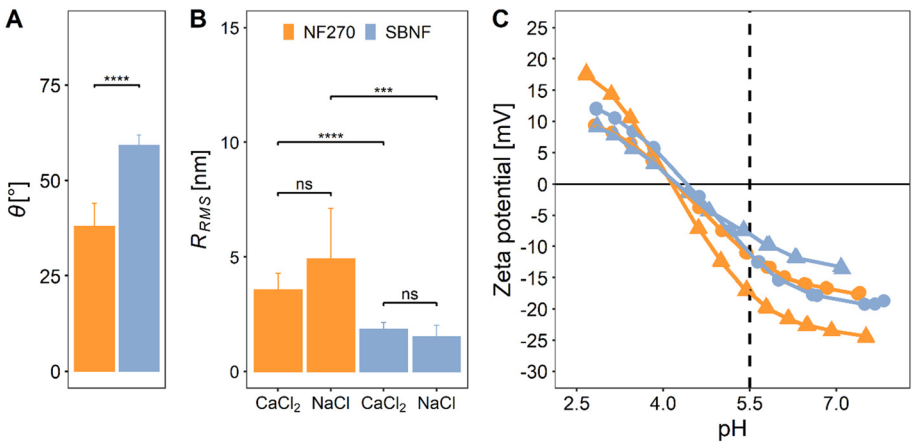

Fig. 1 Contact angle (θ) (A), root-mean-squared roughness (R_{RMS}) (B) and zeta potential (C) of pristine NF270 and SBNF membranes. AFM scans for R_{RMS} determination were obtained in a fluid cell with a monovalent (NaCl) or divalent ($CaCl_2$) electrolyte (n = 15), I = 1 mM, pH = 5.5 (asterisks indicate results from t-tests: **** $p < 0.0001$, *** $p < 0.001$, ns – not significantly different).

Table 1 Interfacial and transport properties of the membranes

Membrane	Active layer material	MWCO [Da]	A_0[c] [LMH per bar]	NaCl rejection[c] [%]	$CaCl_2$ rejection[c] [%]	TOC rejection[c] [%]
NF270	Polypiperazine amide	205–380[a]	8.7 ± 0.7	44.5 ± 7	49.2 ± 5.5	93.5 ± 3.1
SBNF	Cellulose acetate	2000[b]–6000[c]	7.7 ± 1.1	20.4 ± 3.4	24.4 ± 5.3	83.4 ± 4.3

[a] Values from literature.[40,41] [b] Values from manufacturer. [c] Values from this study; LMH – L m^{-2} h^{-1}.

Overall, both membranes are relatively smooth, negatively-charged at the pH of interest and with similar UP water permeance. However, they exhibit significant differences in wettability and rejection attributed to the different active layer polymer chemistries and MWCO, respectively, both of which are expected to contribute to differences in the fouling propensity of the membranes.

3.2. Inorganic fouling and electrostatic double-layer (EDL) repulsion

Inorganic fouling alone resulted in a small flux loss (<5%) for both membrane types (Fig. 2A and C). The presence of divalent ions in solution, *i.e.*, Ca^{2+}, had no effect on Fe oxide fouling. These results can be explained by electrostatic interactions between the foulant and membrane. At low ionic strength (I = 1 mM) and pH 5.5 (bellow the point of zero surface charge), Fe oxide colloids are positively-charged (ζ = 28.4 ± 4.9 mV in 0.3 mM $CaCl_2$ and ζ = 32.1 ± 3.4 in 1 mM NaCl, Fig. S1†) due to Fe–OH_2^+ functional groups on the particle surface,[59] while both membranes have a negative surface charge (Fig. 1C). This can favour initial deposition of a thin foulant layer on the membrane surface due to electrostatic attraction.[45] Following that, the fouling dynamics will be determined by the repulsive interactions between the positively-charged colloids on the membrane surface and those transported from the bulk solution towards the membrane under the permeation drag force. At low ionic

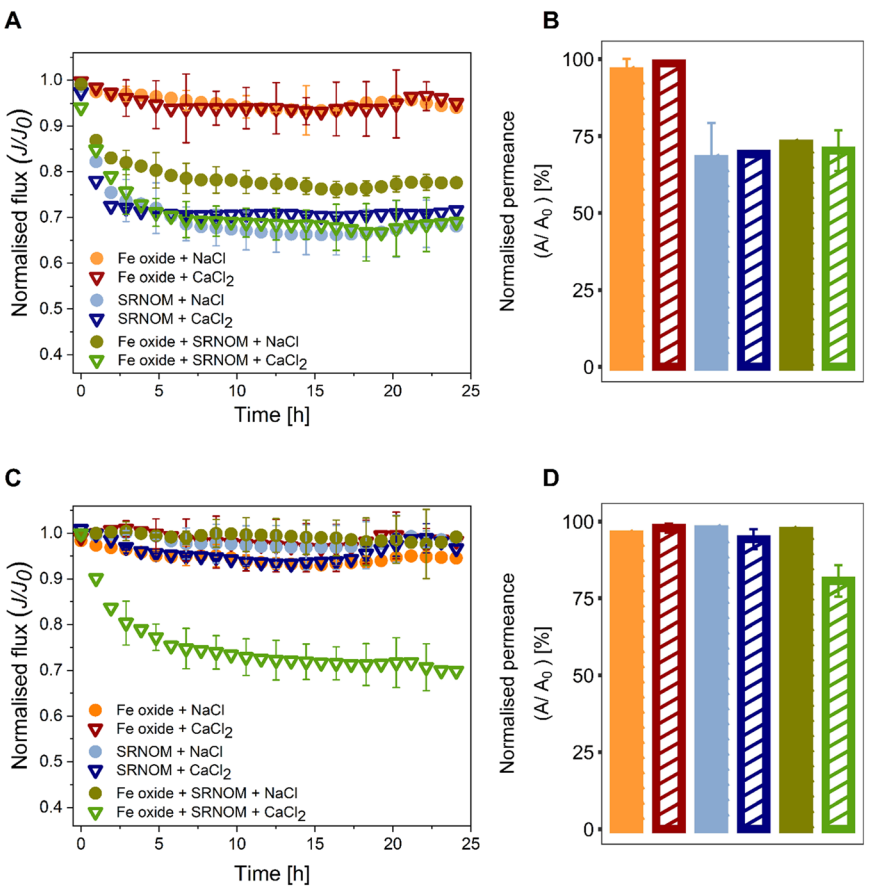

Fig. 2 Normalised flux (J/J_0) over time and normalised permeance (A/A_0) for cellulose acetate (SBNF) (A and B) and polypiperazine amide (NF270) (C and D) membranes during inorganic (40 mg L^{-1} Fe oxide), organic (20 mg C/L SRNOM) and combined (40 mg L^{-1} Fe oxide + 20 mg C/L SRNOM) fouling experiments. Fouling conditions: temperature, T = 20 °C; crossflow velocity, u = 0.23 m s^{-1} (Re = 450); initial flux, J_0 = 100 LMH; pH = 5.5; and ionic strength, I = 1 mM. Each flux decline curve is the average of two replicate experiments, smoothed using the loess function (span = 0.2). Error bars denote the standard deviation between the two unsmoothed replicates.

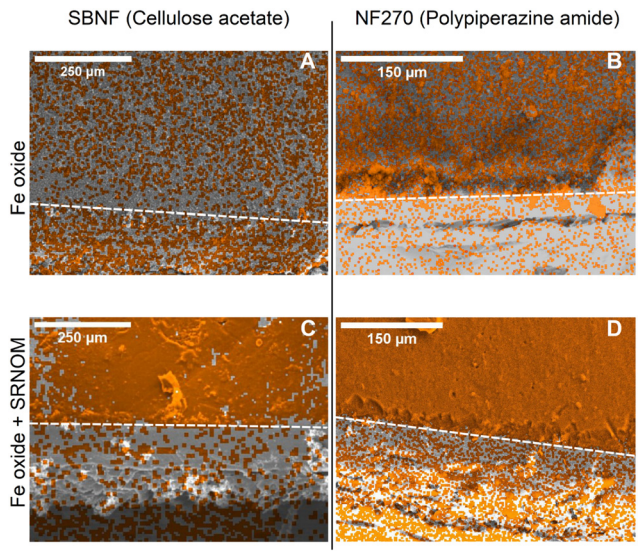

Fig. 3 Elemental maps obtained by energy dispersive X-ray (EDX) analysis, showing iron-rich regions (in orange) overlayed on SEM micrographs of the cross-section and active layer of membranes (tilted 30–60°). Results shown for membranes fouled with: Fe oxide + $CaCl_2$ (A and B for SBNF and NF270, respectively); Fe oxide + SRNOM + $CaCl_2$ (C and D for SBNF and NF270, respectively). White dashed lines indicate the approximate location of the foulant-active layer interface.

strength, electrostatic repulsion between similar charge colloids will be significant, with a calculated Debye length of λ = 9.6 nm for I = 1 mM (see section S3†), hence further deposition will be hindered. This is evident from the thin discontinuous iron-rich layer on the surface of the fouled NF270 and SBNF membrane visible on EDX maps overlayed on SEM micrographs (Fig. 3A and B). Similar results have been observed in smooth cellulose acetate RO membrane fouling experiments with positively-charged aluminium oxide colloids over a range of feed solution ionic strengths (1–100 mM, corresponding to λ = 9.6–0.96 nm). Low flux decline (<10%) was obtained for I < 100 mM, attributing the results to strong repulsive interactions that cannot be overcome by the permeation drag force.[45] Similarly, low flux reduction has been observed in fouling experiments with NF270 membranes and positively-charged aluminium oxide particles at I = 10 mM.[10]

3.3. Organic fouling and hydrophobic interactions

Addition of SRNOM (without Fe oxide) caused significant reduction (28–31%) in the permeate flux of SBNF cellulose acetate membranes after 24-hour filtration (Fig. 2A). Pseudo-steady flux was reached within 2–4 hours of the foulant addition. The NF270 polypiperazine amide membrane was, in contrast, less prone to organic fouling than the cellulose acetate one, showing negligible (<5%) flux decline over the course of the NOM-only experiment (Fig. 2C). The different fouling severity can be explained by the surface and transport properties of the two membranes in combination with the characteristics of the foulant. Previous characterisation studies have shown that the dominant fraction (70%) of the SRNOM is hydrophobic, most of which is hydrophobic acid (*e.g.*, humic and fulvic acids) and hydrophobic neutral.[60] The membrane characterisation showed that the SBNF (cellulose acetate) membrane is more hydrophobic than the NF270 (polypiperazine amide) membrane (Fig. 1A). Strong hydrophobic interactions between the organic foulant and membrane leads to enhanced adsorption of SRNOM onto the SBNF membrane, resulting in higher flux loss.[55] Furthermore, the difference in MWCO between the two membranes, evidenced by the lower TOC rejection of the SBNF membrane (83.4 ± 4.3%) compared to the NF270 membrane (93.5 ± 3.1%) (Table 1), suggests internal blockage as a contributing fouling mechanism for the SBNF membranes. Adsorption of the hydrophobic organic foulant inside the active layer of the hydrophobic SBNF membrane can further exacerbate the flux decline of the cellulose acetate membrane. Although previous studies have shown more severe organic fouling in the presence of divalent ions due to membrane-foulant and foulant-foulant interactions[6,10] enabled by Ca^{2+}, here the salt type did not affect the final flux in NOM-only experiments, with 31% and 28% flux reduction in the presence of NaCl or $CaCl_2$, respectively (Fig. 2A). This further suggests that hydrophobic interactions are of greater importance compared to specific divalent interactions for the cellulose acetate membrane. The discrepancy regarding the effect of divalent ions on fouling between our results and previous research[6,10,27] can be explained by pH effects.[61] At acidic pH (as used in the current study) the foulant and membrane are less negatively charged compared to basic pH (used in previous organic fouling studies with calcium[6,10,27]) (Fig. 1C), as most carboxylic functional groups on the organic foulant will be protonated (–COOH). Concurrently, there will be fewer OH^- groups adsorbed on the SBNF membrane surface conferring upon it a less negative charge (Fig. 1C). The low pH, therefore, has a two-fold effect on fouling severity: lower repulsive foulant-foulant and membrane-foulant interactions, resulting in foulant accumulation at the surface; and fewer negatively-charged sites on the membrane and foulant to participate in specific Ca^{2+} complexation (we show in Fig. S9† that NOM–Ca^{2+} complex formation is mitigated at low pH), leading to similar flux decline regardless of ion type. This has been confirmed experimentally in nanofiltration of SRHA at different pH.[61] At a fixed ionic strength (10 mM), in alkaline solution (pH 8) there was a significant difference in the flux loss with added divalent cations (17%) compared to that in their absence (2%).[61] Whereas there was no effect of divalent ions at pH 4, where the flux declined by 14% in the presence of Na^+, and 11% with added Ca^{2+}. Based on this previous research, we speculate that the flux decline during SRNOM organic fouling in the presence of divalent ions at pH of 6–7.5, typical for surface water,[11,12,62] would be of a comparable magnitude to the one we observe at pH 5.5. However, the underlying mechanisms would differ, with calcium complexation and gel formation becoming dominant at or above near-neutral pH.[27,61]

3.4. Combined fouling – interplay between membrane and foulant properties

The combined Fe oxide + SRNOM fouling resulted in a 20% flux decline in the presence of NaCl and 30% flux decline with the addition of $CaCl_2$ for the SBNF (Fig. 2A). This can again be linked to the properties of the feed foulant and membrane surface characteristics. In the presence of SRNOM in the feed solution, organics adsorb onto the colloids causing the positively-charged Fe oxide to undergo charge reversal: from 32.1 mV to −33.1 mV in 1 mM NaCl and from 28.4 mV to −17.9 mV in 0.3 mM $CaCl_2$ (Fig. S1†).[25,34] Thus, SBNF membrane fouling will be driven by hydrophobic interactions due to SRNOM coating the Fe oxide colloids. In contrast, for the less hydrophobic membrane (polypiperazine amide NF270), the main determinant of combined (Fe oxide + SRNOM) fouling is the presence of Ca^{2+}. As shown in Fig. 2C, the NF270 membrane experienced more severe flux reduction, 29%, during the combined (Fe oxide + SRNOM) fouling in the presence of calcium ions compared to that with added sodium ions (Fig. 2C). The difference in the fouling behaviour can be explained by changes in the feed foulant surface charge. The NOM-coated Fe oxide colloids are less negatively charged in a Ca-containing dispersion (ζ = −17.9 ± 2.1 mV) compared to a Na-containing dispersion (ζ = −33.1 ± 4.7 mV) (Fig. S1†), leading to a lower energy barrier for colloids deposition on the membrane. Calculations of the electrostatic double-layer repulsive force (F_{EDL}) demonstrate that a change in the colloid surface charge from −33 mV to −18 mV reduces the F_{EDL} almost three times, when all other solution parameters are kept the same (*cf.* S3 of the ESI†). Similarly, a modelling study investigating the effect of zeta potential on colloidal fouling has confirmed that lowering the foulant zeta potential from 30 mV to 20 mV, leads to two times more flux decline.[63] This has been attributed to the lower energy barrier that particles need to overcome to deposit on the membrane surface at lower zeta potential: 2.20 k_BT and 5.22 k_BT (k_B is Boltzmann's constant) for ζ = 20 mV and ζ = 30 mV, respectively.[63] A lower F_{EDL} in the presence of Ca^{2+} also underlies the greater extent of fouling in combined (Fe oxide + SRNOM) experiments using SBNF membranes (Fig. 2A). The lower absolute surface zeta potential can be linked to adsorption of divalent ions onto the NOM-coated Fe oxide colloids through competitive adsorption of ions onto hydrophobic neutral sites,[55] as well as site-binding of cations onto negatively-charged hydrophilic sites.[55] In both cases, adsorption of Ca^{2+} onto the NOM-coated colloids will increase the number of positively-charged surface sites compared to adsorption of Na^+ due to the higher valence of calcium. The severe flux loss during combined fouling experiments (Fe oxide + SRNOM) in the presence of Ca^{2+} ions, owing to the lower magnitude of ζ in the presence of divalent ions is also consistent with the continuous iron-rich layer on the membrane surface (Fig. 3C and D and S10†).

In summary, the flux loss data suggests that hydrophobic interactions along with the higher MWCO of cellulose acetate active layer explain the extent of organic and combined fouling for the SBNF membrane, while electrostatic interactions (modulated by NOM and Ca^{2+}) are responsible for the flux decline observed for the NF270 membranes during the combined organic–inorganic fouling in the presence of $CaCl_2$. We expect that at higher pH of 6–7.5, typical for surface water,[11,12,62] the cellulose acetate membrane would remain more susceptible to fouling due to hydrophobic organic substances, as a result of its higher contact angle compared to the polypiperazine amide membrane (Fig. 1C). Although pH can have an effect on the hydrophobicity of a material, it has been show for a number of commercial polymeric NF membranes that this change is only significant at extreme pH (pH $<$ 4 and pH $>$ 8).[64] Further support of the dominant fouling mechanisms for the two membranes is provided in the next section, where the ion rejection over the course of the fouling is discussed.

3.5. Effect of foulant and membrane type on ion (NaCl or $CaCl_2$) rejection

Ion rejection was measured before the onset of fouling (pristine membrane), during fouling (at 1.5 h, 20 h and 23.5 h) and after 15-minute UP-water cleaning (Fig. 4). The pristine SBNF membrane had lower rejection (20.4 ± 3.4% and 24.4 ± 5.3% for NaCl and $CaCl_2$, respectively) compared to the NF270 (44.5 ± 7.0% and 49.2 ± 5.5% for NaCl and $CaCl_2$, respectively), consistent with the higher MWCO of SBNF (Table 1). The TOC rejection did not change significantly over the course of the organic and combined fouling experiments (Fig. S11†).

The SBNF membrane experienced an increase in the NaCl and $CaCl_2$ rejection during fouling compared to the initial rejection of the pristine membrane (Fig. 4A), with rejection increasing roughly twofold (from ~22% to 40–55%) for the organic and combined fouling experiments. The improvement in rejection of both salts is due to the severe fouling (including internal fouling) exhibited by SBNF (Fig. 2A): the loose hydrophobic SBNF membrane can experience adsorption of organic foulant inside the active layer, leading to blockage and hindered transport of ions through the membrane. Charge exclusion mechanisms do not seem to play a role, as the rejection increase was not salt-dependent. On the other hand, the inorganic fouling caused a small rejection increase from 19% to 22% for the NaCl; and from 25% to 36% for $CaCl_2$ (Fig. 4A), while resulting in small flux reduction (Fig. 2A). This is consistent with the discontinuous foulant layer observed on the membrane surface during Fe oxide fouling, which suggests that there is little obstruction to ion transport (Fig. 3A).

For the NF270 membrane, the change in salt rejection during fouling depended on the type of foulant and retained ion (Fig. 4B). There was no significant change in rejection of NaCl or $CaCl_2$ between the pristine membrane and that

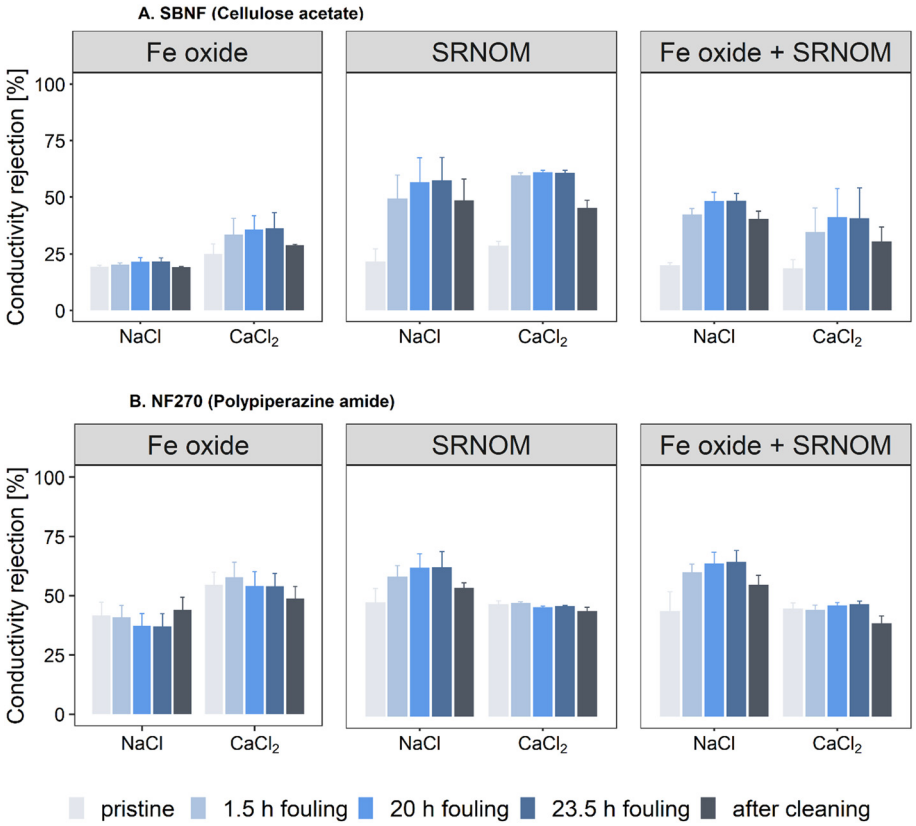

Fig. 4 Conductivity rejection of pristine, fouled (1.5 h, 20 h and 23.5 h) and cleaned (15-minute UP water cleaning; u = 0.23 m s^{-1}, Re = 450) cellulose acetate (SBNF) (A) and polypiperazine amide (NF270) (B) membranes during inorganic (40 mg L^{-1} Fe oxide), organic (20 mg C/L SRNOM) and mixed (40 mg L^{-1} Fe oxide + 20 mg C/L SRNOM) fouling experiments. Fouling conditions: temperature (T = 20 °C), crossflow velocity (u = 0.23 m s^{-1}, Re = 450), initial flux (J_0 = 100 LMH), pH = 5.5 and ionic strength (I = 1 mM). Error bars indicate standard deviation of measurements from two replicate experiments.

fouled with the Fe oxide (Fig. 4B). In the presence of SRNOM (with or without Fe oxide), the $CaCl_2$ rejection remained unchanged (<5% change) throughout the fouling, while the NaCl rejection increased from 48% to 62% (SRNOM alone) and from 44% to 65% (combined fouling) after 23.5 hours of fouling when compared to the pristine membrane rejection (Fig. 4B). This suggests that charge interactions play an important role during salt rejection of NOM fouled membranes. Notably, NaCl rejection was higher than that for $CaCl_2$ during the organics-containing fouling experiments. The differences in transport of monovalent and divalent ions have been extensively studied for NF membranes[30,65–67] and are due to the interplay between membrane MWCO and ion rejection by steric (size) exclusion, Donnan (charge) exclusion and dielectric effects (*e.g.*, higher solvation energy barrier at the solvent-membrane interface).[65,68] The dominant ion rejection mechanism for NF membranes is often assumed to be size exclusion, which ensures higher rejection with increasing ion size.[66] However, Donnan effects between charged foulant and membrane (fouled or pristine) can also be significant.[49,66,67] Previous studies that have reported lower rejection of a divalent salt ($MgCl_2$ or $CaCl_2$) compared to monovalent (NaCl) salt for NF membranes attribute the results to the stronger attraction between a divalent ion and oppositely-charged membrane, compared to that with a monovalent one, which enhances the passage of the higher valence ions through the membrane.[49,66,67] It appears likely that the lower Ca^{2+} rejection in the SRNOM-fouled membranes is due to enhanced ion partitioning facilitated by the negatively-charged SRNOM at the surface.

3.6. Fouling severity and dominant fouling mechanisms

Fouling reversibility through hydraulic cleaning, *i.e.* hydraulically reversible fouling, was assessed for all investigated systems by circulating UP water for 15-minutes (u = 0.23 m s^{-1}, Re = 450, TMP = 0 bar). For the cases where severe flux decline was observed, *i.e.*, organic and combined fouling for the SBNF membrane and combined fouling in the presence of $CaCl_2$ for the NF270 membrane (Fig. 2A and C), the permeance could not be fully restored using 15-minute UP water cleaning (Fig. 2B and D). In the cases of significant flux decline with the SBNF membrane, the final permeance after cleaning (A) varied between 68% and 73% of the initial pristine membrane permeance (A_0) (Fig. 2B). In the particular case of combined fouling in the presence of $CaCl_2$, although the polypiperazine amide and cellulose acetate membranes experienced a similar flux loss of ≈30%, the NF270

permeance was recovered to a greater extent (A/A_0 = 80%) compared to the SBNF membrane (A/A_0 = 70%) (Fig. 2B and D). The lower permeance recovery for the SBNF membrane after cleaning compared to the NF270 further suggests that stronger hydrophobic interactions and internal organic fouling (which is not removed by hydraulic surface cleaning to a significant extent) are the dominant mechanisms governing the flux loss experienced by the cellulose acetate membrane. Furthermore, the conductivity rejection after cleaning did not return to that of the pristine SBNF membrane and remained at twice the value of the pristine membrane (Fig. 4A), again showing inefficient removal of fouling using hydraulic surface cleaning. This observation was more pronounced for the cases with severe flux loss and significant rejection increase during filtration (*e.g.*, organic and combined fouling), which further supports severe internal foulant deposition as a dominant fouling mechanism of the SBNF membranes.

4. Conclusion

In this paper, we have shown that organic (SRNOM) and combined (Fe oxide + SRNOM) fouling led to significant and hydraulically irreversible change in the flux and ion rejection of the cellulose acetate (SBNF) membrane. In contrast, the polypiperazine amide (NF270) membrane was less prone to fouling, suggesting this polymer would be preferred over cellulose acetate for the treatment of organic-rich waters (with or without iron). Hydrophobic interactions along with the higher MWCO of the cellulose acetate explain the more significant effect of organic and combined fouling of the SBNF, while weaker electrostatic repulsive interactions (due to Ca^{2+} adsorption on NOM-coated Fe oxide) are responsible for the flux decline observed in the polypiperazine amide membranes during the combined fouling in the presence of $CaCl_2$. Studying systematically the effect of surface water composition on membrane flux in laboratory experiments is imperative for identifying and limiting the precursors of fouling. Our results show that NOM is the main precursor of fouling, with Fe oxide playing a secondary role as a substrate for NOM sorption; therefore pre-treatment and cleaning-in-place protocols need to target organic foulants. We explain the governing fouling mechanisms by linking the geochemical behaviour of positively-charged colloids in the presence of NOM (*i.e.*, charge reversal) to membrane surface properties (*e.g.* charge and hydrophobicity). Given the significant decrease in the absolute charge of the combined foulant in the presence of divalent (Ca^{2+}) compared to monovalent (Na^{+}) ions, along with the calculated reduction in electrostatic double-layer repulsive foulant-foulant interaction force (F_{EDL}), future experiments with higher valence naturally-occurring ions (such as Al^{3+}) should be conducted to fully understand the foulant-membrane and foulant–foulant charge interactions. Furthermore, a complex background electrolyte solutions (combining a mix of monovalent and multivalent ions: Na^{+}, Ca^{2+}, Al^{3+}) should be used in future research to reflect more realistic feed water matrices. Finally, studies monitoring the long-term operation of full-scale membrane DWTPs are necessary to establish which foulants are causally responsible for permeate flux and quality deterioration, while also taking into account seasonal variations in water quality and temperature.

Conflicts of interest

The authors declare no competing financial interest.

Acknowledgements

The authors would like to thank Scottish Water for the funds awarded to Dr. Andrea Semiao; and the EPSRC (supported by Scottish Water) for the PhD studentship (EP/R513209/1(2383022)) awarded to Desislava Davidkova. The authors would like to thank Dr. Laura Charlton for the AFM image acquisition. The authors would like to acknowledge the use of the Cryo FIB/SEM facility (Zeiss Crossbeam 550) bought with EPSRC grant EP/P030564/1 and the training and help provided by Dr Fraser Laidlaw for SEM image acquisition. The authors would like to thank Prof Xuan Zhang from the Nanjing University of Science and Technology for conducting the streaming potential measurements.

References

1 A. W. Mohammad, Y. H. Teow, W. L. Ang, Y. T. Chung, D. L. Oatley-Radcliffe and N. Hilal, Nanofiltration membranes review: Recent advances and future prospects, *Desalination*, 2015, **356**, 226–254.
2 M. Jafari, M. Vanoppen, J. M. C. van Agtmaal, E. R. Cornelissen, J. S. Vrouwenvelder and A. Verliefde, *et al.*, Cost of fouling in full-scale reverse osmosis and nanofiltration installations in the Netherlands, *Desalination*, 2021, **500**, 114865.
3 Y. Guo, T. Yu. Li, K. Xiao, X. M. Wang and Y. F. Xie, Key foulants and their interactive effect in organic fouling of nanofiltration membranes, *J. Membr. Sci.*, 2020, **610**, 118252.
4 C. Y. Tang, T. H. Chong and A. G. Fane, Colloidal interactions and fouling of NF and RO membranes: A review, *Adv. Colloid Interface Sci.*, 2011, **164**(1–2), 126–143.
5 H. Yu, X. Li, H. Chang, Z. Zhou, T. Zhang and Y. Yang, *et al.*, Performance of hollow fiber ultrafiltration membrane in a full-scale drinking water treatment plant in China: A systematic evaluation during 7-year operation, *J. Membr. Sci.*, 2020, **613**, 118469.
6 S. Lee, J. Cho and M. Elimelech, Combined influence of natural organic matter (NOM) and colloidal particles on nanofiltration membrane fouling, *J. Membr. Sci.*, 2005, **262**(1–2), 27–41.
7 Q. Li and M. Elimelech, Synergistic effects in combined fouling of a loose nanofiltration membrane by colloidal materials and natural organic matter, *J. Membr. Sci.*, 2006, **278**(1–2), 72–82.

8 A. E. Contreras, A. Kim and Q. Li, Combined fouling of nanofiltration membranes: Mechanisms and effect of organic matter, *J. Membr. Sci.*, 2009, **327**(1–2), 87–95.
9 T. O. Mahlangu, J. M. Thwala, B. B. Mamba, A. D'Haese and A. R. D. Verliefde, Factors governing combined fouling by organic and colloidal foulants in cross-flow nanofiltration, *J. Membr. Sci.*, 2015, **491**, 53–62.
10 T. O. Mahlangu, E. M. V. Hoek, B. B. Mamba and A. R. D. Verliefde, Influence of organic, colloidal and combined fouling on NF rejection of NaCl and carbamazepine: Role of solute–foulant–membrane interactions and cake-enhanced concentration polarisation, *J. Membr. Sci.*, 2014, **471**, 35–46.
11 W. R. Bowen, T. A. Doneva and H. B. Yin, Separation of humic acid from a model surface water with PSU/SPEEK blend UF/NF membranes, *J. Membr. Sci.*, 2002, **206**(1–2), 417–429.
12 C. Vergel, R. N. Franks, C. Bartels and M. Neculau, A nanofiltration membrane for the removal of color from surface water to meet Norwegian standards, *Desalin. Water Treat.*, 2017, **85**, 6–15.
13 L. Durand-Bourlier, A. Tinghir, P. Masereel and S. Baig, Nanofiltration selection for NOM removal: Pilot and full-scale operation, *Water Pract. Technol.*, 2011, **6**, 2011026.
14 W. Davison, Iron and manganese in lakes, *Earth-Sci. Rev.*, 1993, **34**(2), 119–163.
15 C. Patterson, M. Asce, A. Anderson, R. Sinha, N. Muhammad and D. Pearson, Nanofiltration Membranes for Removal of Color and Pathogens in Small Public Drinking Water Sources, *J. Environ. Eng.*, 2012, **138**(1), 48–57.
16 B. Ericsson, M. Hallberg and J. Wachenfeldt, Nanofiltration of highly colored raw water for drinking water production, *Desalination*, 1996, **108**(1–3), 129–141.
17 S. Sutherland, S. A. Parsons, A. Daneshkhah, P. Jarvis and S. J. Judd, THM precursor rejection by UF membranes treating Scottish surface waters, *Sep. Purif. Technol.*, 2015, **149**, 381–388.
18 M. Luo and Z. Wang, Complex fouling and cleaning-in-place of a reverse osmosis desalination system, *Desalination*, 2001, **141**(1), 15–22.
19 D. C. Sioutopoulos, S. G. Yiantsios and A. J. Karabelas, Relation between fouling characteristics of RO and UF membranes in experiments with colloidal organic and inorganic species, *J. Membr. Sci.*, 2010, **350**(1–2), 62–82.
20 R. D. Cohen and R. F. Probstein, Colloidal fouling of reverse osmosis membranes, *J. Colloid Interface Sci.*, 1986, **114**(1), 194–207.
21 T. A. Clair, I. F. Dennis, R. Vet and H. Laudon, Long-term trends in catchment organic carbon and nitrogen exports from three acidified catchments in Nova Scotia, Canada, *Biogeochemistry*, 2008, **87**(1), 83–97.
22 M. Valdivia-Garcia, P. Weir, D. W. Graham and D. Werner, Predicted Impact of Climate Change on Trihalomethanes Formation in Drinking Water Treatment, *Sci. Rep.*, 2019, **9**(1), 1–10.
23 J. Vuorenmaa, M. Forsius and J. Mannio, Increasing trends of total organic carbon concentrations in small forest lakes in Finland from 1987 to 2003, *Sci. Total Environ.*, 2006, **365**(1–3), 47–65.
24 L. E. Anderson, B. F. Trueman, D. W. Dunnington and G. A. Gagnon, Relative importance of organic- and iron-based colloids in six Nova Scotian lakes, *npj Clean Water*, 2021, **4**(1), 1–10.
25 A. Philippe and G. E. Schaumann, Interactions of Dissolved Organic Matter with Natural and Engineered Inorganic Colloids: A Review, *Environ. Sci. Technol.*, 2014, **48**(16), 8946–8962.
26 S. Lee and M. Elimelech, Relating organic fouling of reverse osmosis membranes to intermolecular adhesion forces, *Environ. Sci. Technol.*, 2006, **40**(3), 980–987.
27 Q. Li and M. Elimelech, Organic fouling and chemical cleaning of nanofiltration membranes: Measurements and mechanisms, *Environ. Sci. Technol.*, 2004, **38**(17), 4683–4693.
28 C. Moens, N. Waegeneers, A. Fritzsche, P. Nobels and E. Smolders, A systematic evaluation of Flow Field Flow Fractionation and single-particle ICP-MS to obtain the size distribution of organo-mineral iron oxyhydroxide colloids, *J. Chromatogr. A*, 2019, **1599**, 203–214.
29 DWI. LIST OF APPROVED PRODUCTS FOR USE IN PUBLIC WATER SUPPLY IN THE UNITED KINGDOM [Internet]. 2023. Available from: **https://dwi-content.s3.eu-west-2.amazonaws.com/wp-content/uploads/2021/05/20152135/SoS_list_May23.pdf**.
30 C. Boo, Y. Wang, I. Zucker, Y. Choo, C. O. Osuji and M. Elimelech, High Performance Nanofiltration Membrane for Effective Removal of Perfluoroalkyl Substances at High Water Recovery, *Environ. Sci. Technol.*, 2018, **52**(13), 7279–7288.
31 C. Y. Tang, Y. N. Kwon and J. O. Leckie, Fouling of reverse osmosis and nanofiltration membranes by humic acid-Effects of solution composition and hydrodynamic conditions, *J. Membr. Sci.*, 2007, **290**(1–2), 86–94.
32 W. S. Ang, A. Tiraferri, K. L. Chen and M. Elimelech, Fouling and cleaning of RO membranes fouled by mixtures of organic foulants simulating wastewater effluent, *J. Membr. Sci.*, 2011, **376**, 196–206.
33 S. Lee and M. Elimelech, Salt cleaning of organic-fouled reverse osmosis membranes, *Water Res.*, 2007, **41**(5), 1134–1142.
34 Y. Zhang, Y. Chen, P. Westerhoff and J. Crittenden, Impact of natural organic matter and divalent cations on the stability of aqueous nanoparticles, *Water Res.*, 2009, **43**(17), 4249–4257.
35 H. Fu, K. Liu, P. J. J. Alvarez, D. Yin, X. Qu and D. Zhu, Quantifying hydrophobicity of natural organic matter using partition coefficients in aqueous two-phase systems, *Chemosphere*, 2019, **218**, 922–929.
36 D. J. Burleson and R. L. Penn, Two-Step Growth of Goethite from Ferrihydrite, *Langmuir*, 2006, **22**(1), 402–409.
37 S. Lee, J. Cho and M. Elimelech, Influence of colloidal fouling and feed water recovery on salt rejection of RO and NF membranes, *Desalination*, 2004, **160**(1), 1–12.
38 W. S. Ang, S. Lee and M. Elimelech, Chemical and physical aspects of cleaning of organic-fouled reverse osmosis membranes, *J. Membr. Sci.*, 2006, **272**(1–2), 198–210.

39 W. S. Ang, N. Y. Yip, A. Tiraferri and M. Elimelech, Chemical cleaning of RO membranes fouled by wastewater effluent: Achieving higher efficiency with dual-step cleaning, *J. Membr. Sci.*, 2011, **382**(1–2), 100–106.
40 B. M. Xaba, S. J. Modise, B. J. Okoli, M. E. Monapathi and S. Nelana, Characterization of selected polymeric membranes used in the separation and recovery of palladium-based catalyst systems, *Membranes*, 2020, **10**(8), 1–21.
41 L. Gao, H. Wang, Y. Zhang and M. Wang, Nanofiltration membrane characterization and application: Extracting lithium in lepidolite leaching solution, *Membranes*, 2020, **10**(8), 1–18.
42 S. BinAhmed, R. M. Hozalski and S. Romero-Vargas Castrillón, Feed Temperature Effects on Organic Fouling of Reverse Osmosis Membranes: Competition of Interfacial and Transport Properties, *ACS ES&T Engg*, 2021, **1**(3), 591–602.
43 F. Qu, H. Liang, Z. Wang, H. Wang, H. Yu and G. Li, Ultrafiltration membrane fouling by extracellular organic matters (EOM) of Microcystis aeruginosa in stationary phase: Influences of interfacial characteristics of foulants and fouling mechanisms, *Water Res.*, 2012, **46**(5), 1490–1500.
44 J. Cho, G. Amy, J. Pellegrino and Y. Yoon, Characterization of clean and natural organic matter (NOM) fouled NF and UF membranes, and foulants characterization, *Desalination*, 1998, **118**(1–3), 101–108.
45 X. Zhu and M. Elimelech, Fouling of Reverse Osmosis Membranes by Aluminum Oxide Colloids, *J. Environ. Eng.*, 1995, **121**(12), 884–892.
46 L. D. Nghiem, D. Vogel and S. Khan, Characterising humic acid fouling of nanofiltration membranes using bisphenol A as a molecular indicator, *Water Res.*, 2008, **42**(15), 4049–4058.
47 L. Pino-Soto, A. Schwarz, C. Vargas, F. Saravia, H. Horn and R. Bórquez, Influence of multivalent-electrolyte metal solutions on the superficial properties and performance of a polyamide nanofiltration membrane, *Sep. Purif. Technol.*, 2021, **272**, 118846.
48 Z. Chen, J. Luo, X. Hang and Y. Wan, Physicochemical characterization of tight nanofiltration membranes for dairy wastewater treatment, *J. Membr. Sci.*, 2018, **547**, 51–63.
49 C. L. Ritt, J. R. Werber, M. Wang, Z. Yang, Y. Zhao and H. J. Kulik, *et al.*, Ionization behavior of nanoporous polyamide membranes, *Proc. Natl. Acad. Sci. U. S. A.*, 2020, **117**(48), 30191–30200.
50 S. Wang, Z. Y. Wang, J. Z. Xia and X. M. Wang, Polyethylene-supported nanofiltration membrane with *in situ* formed surface patterns of millimeter size in resisting fouling, *J. Membr. Sci.*, 2021, **620**, 118830.
51 S. Gopi, A. Pius, R. Kargl, K. S. Kleinschek and S. Thomas, Fabrication of cellulose acetate/chitosan blend films as efficient adsorbent for anionic water pollutants, *Polym. Bull.*, 2019, **76**(3), 1557–1571.
52 T. Białopiotrowicz and B. Jańczuk, The wettability of a cellulose acetate membrane in the presence of bovine serum albumin, *Appl. Surf. Sci.*, 2002, **201**(1–4), 146–153.
53 A. E. Childress and J. A. Brant, Desalination and Water Purification Research and Development Program No. 57: Characterization of the Hydrophobicity of Polymeric Reverse Osmosis and Nanofiltration Membranes: Implications to Membrane Fouling [Internet]. 2000 [cited 2022 Aug 17]. Available from: **https://www.usbr.gov/pmts/water/publications/reports.html**.
54 X. Zhu and M. Elimelech, Colloidal fouling of reverse osmosis membranes: Measurements and fouling mechanisms, *Environ. Sci. Technol.*, 1997, **31**(12), 3654–3662.
55 L. Bruni and S. Bandini, The role of the electrolyte on the mechanism of charge formation in polyamide nanofiltration membranes, *J. Membr. Sci.*, 2008, **308**(1–2), 136–151.
56 A. Akbari, S. E. Meragawi, S. T. Martin, B. Corry, E. Shamsaei and C. D. Easton, *et al.*, Solvent Transport Behavior of Shear Aligned Graphene Oxide Membranes and Implications in Organic Solvent Nanofiltration, *ACS Appl. Mater. Interfaces*, 2018, **10**(2), 2067–2074.
57 T. O. Mahlangu, T. A. M. Msagati, E. M. V. Hoek, A. R. D. Verliefde and B. B. Mamba, Rejection of pharmaceuticals by nanofiltration (NF) membranes: Effect of fouling on rejection behaviour, *Phys. Chem. Earth*, 2014, **76–78**, 28–34.
58 Y. Wang, I. Zucker, C. Boo and M. Elimelech, Removal of Emerging Wastewater Organic Contaminants by Polyelectrolyte Multilayer Nanofiltration Membranes with Tailored Selectivity, *ACS ES&T Engg*, 2021, **1**(3), 404–414.
59 E. Illés and E. Tombácz, The effect of humic acid adsorption on pH-dependent surface charging and aggregation of magnetite nanoparticles, *J. Colloid Interface Sci.*, 2006, **295**(1), 115–123.
60 T. Ratpukdi, J. A. Rice, G. Chilom, A. Bezbaruah and E. Khan, Rapid Fractionation of Natural Organic Matter in Water Using a Novel Solid-Phase Extraction Technique, *Water Environ. Res.*, 2009, **81**(11), 2299–2308.
61 S. Hong and M. Elimelech, Chemical and physical aspects of natural organic matter (NOM) fouling of nanofiltration membranes, *J. Membr. Sci.*, 1997, **132**(2), 159–181.
62 M. Valdivia-Garcia, P. Weir, Z. Frogbrook, D. W. Graham and D. Werner, Climatic, Geographic and Operational Determinants of Trihalomethanes (THMs) in Drinking Water Systems, *Sci. Rep.*, 2019, **6**(1), 1–12.
63 J. Liu, Y. Fan, Y. Sun, Z. Wang, D. Zhao and T. Li, *et al.*, Modelling the critical roles of zeta potential and contact angle on colloidal fouling with a coupled XDLVO - collision attachment approach, *J. Membr. Sci.*, 2021, **623**, 119048.
64 M. Mänttäri, A. Pihlajamäki and M. Nyström, Effect of pH on hydrophilicity and charge and their effect on the filtration efficiency of NF membranes at different pH, *J. Membr. Sci.*, 2006, **280**(1–2), 311–320.
65 Y. Roy, D. M. Warsinger and J. H. Lienhard, Effect of temperature on ion transport in nanofiltration membranes: Diffusion, convection and electromigration, *Desalination*, 2017, **420**, 241–257.
66 B. Van Der Bruggen, A. Koninckx and C. Vandecasteele, Separation of monovalent and divalent ions from aqueous

solution by electrodialysis and nanofiltration, *Water Res.*, 2004, **38**(5), 1347–1353.

67 T. Zhang, Z. H. He, K. P. Wang, X. M. Wang, Y. F. F. Xie and L. Hou, Loose nanofiltration membranes for selective rejection of natural organic matter and mineral salts in drinking water treatment, *J. Membr. Sci.*, 2022, **662**, 120970.

68 J. Luo and Y. Wan, Effects of pH and salt on nanofiltration-a critical review, *J. Membr. Sci.*, 2013, **438**, 18–28.